Hepatology Publish Ahead of Print
DOI:10.1097/HEP.0000000000000523

OPEN

LANCL1, a cell-surface protein, promotes liver tumor initiation via FAM49B-Rac1 axis to suppress oxidative stress

Hongyang Huang[1,2,#], Yu-Man Tsui[1,2,#], Daniel Wai-Hung Ho[1,2], Clive Yik-Sham Chung[1,3], Karen Man-Fong Sze[1,2], Eva Lee[1,2], Gary Cheuk-Hang Cheung[1,2], Vanilla Xin Zhang[1,2], Xia Wang[1,2], Xueying Lyu[1,2], Irene Oi-Lin Ng[1,2,*]

[1]Department of Pathology, The University of Hong Kong, Hong Kong

[2]State Key Laboratory of Liver Research, The University of Hong Kong, Hong Kong

[3]School of Biomedical Sciences, The University of Hong Kong, Hong Kong

Keywords: Extracellular N-terminal region, reactive oxygen species (ROS), sphere formation, tumorigenicity, translational applications

#Contributed equally.

*Corresponding Author: Irene Oi-Lin Ng, Room 7-13, Block T, Queen Mary Hospital, Pokfulam, Hong Kong; Tel: 22552664; Fax: 28725197; E-mail: iolng@hku.hk.

List of abbreviations:

HCC, hepatocellular carcinoma; DMEM-HG, Dulbecco's Modified Eagle Medium-high glucose; FBS, fetal bovine serum; P/S, penicillin-streptomycin cocktail; NaPy, sodium pyruvate; qPCR, real-time quantitative PCR; T, tumor; NTL, non-tumorous liver; RNA-seq, RNA-sequencing; NTC, non-target control; KD, knockdown; IF, immunofluorescence; LANCL1, lanthionine synthase C-like protein 1; WT, wild-type; TICs, tumor initiating cells; 5-FU, 5-fluorouracil; ROS, reactive oxygen species; GSEA, gene set enrichment analysis; NAC, N-acetylcysteine; GSH, glutathione; TBHP, tert-Butyl hydroperoxide; Co-IP, co-immunoprecipitation; NOXs, NADPH oxidases; CHX, cycloheximide; Nrf2: nuclear factor (erythroid-derived 2) factor 2; Keap1, Kelch-like ECH associated protein 1; GCLC, glutamate-cysteine ligase catalytic subunit.

Financial support: The study was supported by the Hong Kong Research Grants Council Theme-based Research Scheme (T12-704/16-R and T12-716/22-R), Innovation and Technology Commission grant to State Key Laboratory of Liver Research (ITC PD/17-9), National Natural Science Foundation of China (81872222 and 82203234), and University Development Fund of The University of Hong Kong. I.O.L. Ng is Loke Yew Professor in Pathology.

Graphic abstract

GA1

Abstract

Background & Aims: Hepatocellular carcinoma (HCC) is an aggressive cancer with a poor clinical outcome. Understanding the mechanisms that drive tumor initiation is important for improving treatment strategy. This study aimed to identify functional cell membrane proteins that promote HCC tumor initiation.

Approach & Results: Tailor-made siRNA library screening was performed for all membrane protein-encoding genes that are upregulated in human HCC (n=134), with sphere formation as surrogate readout for tumor initiation. Upon confirmation on membranous localization by immunofluorescence and tumor initiation ability by limiting dilution assay in vivo, LanC-like protein-1 (LANCL1) was selected for further characterization. LANCL1 suppressed intracellular reactive oxygen species (ROS) and promoted tumorigenicity both in vitro and in vivo. Mechanistically, with mass spectrometry, FAM49B was identified as a downstream binding partner of LANCL1. LANCL1 stabilized FAM49B by blocking the interaction of FAM49B with the specific E3 ubiquitin ligase TRIM21, thus protecting FAM49B from ubiquitin-proteasome degradation. LANCL1-FAM49B axis suppressed the Rac1-NADPH oxidase (NOX)-driven ROS production but this suppression of ROS was independent of the GSH transferase function of LANCL1. Clinically, HCCs with high co-expression of LANCL1 and FAM49B were associated with more advanced tumor stage, poorer overall survival and disease-free survival. In addition, anti-LANCL1 antibodies targeting the extracellular N-terminal domain were able to suppress the self-renewal ability as demonstrated by the sphere formation ability of HCC cells.

Conclusions: Our data showed that LANCL1 is a cell-surface protein and a key contributor to HCC initiation. Targeting the LANCL1-FAM49B-Rac1-NOX-ROS signaling axis may be a promising therapeutic strategy for HCC.

Hepatocellular carcinoma (HCC) is a prevalent malignancy worldwide. Although surgical resection and liver transplantation offer a potential cure, most HCCs are diagnosed at advanced stages and thus inoperable. Even if operated, the tumor recurrence rate is high. HCC is notoriously resistant to conventional chemotherapy, hence treatments for advanced HCC are limited. Tumor initiation is crucial in both hepatocarcinogenesis and tumor recurrence by residual tumor cell population after treatment. Understanding the mechanisms that drive tumor initiation is important for improving treatment strategy (1).

Cell surface proteins are top-ranking candidates for targeted therapy development due to the ease of targeting. Targeting specific cell surface functional proteins that trigger specific cell signaling pathways in tumor initiation will offer a promising option in therapy. So far, several cell surface proteins that promote liver tumor initiation have been identified. These include CD13(2), CD24(3), CD47(4), CD90(5), CD133(6), and EpCAM(7). However, we and others have demonstrated the limitations of some of these proteins in translational applications. For instance, some of them have low expression in terms of either a very low percentage of positive cells in a tumor or very few patients' samples showing detectable expression (such as CD90)(8), implicating a lesser role of the protein in HCC initiation in certain cohort of patients. Also, some surface proteins are detectable not only in HCC tumors but also at high levels in non-tumorous liver tissues. Targeting these proteins may cause a non-specific cytotoxic effect on the surrounding non-tumorous liver tissues. There is an urgent need to identify new,

functional cell surface proteins that are responsible for driving liver tumor initiation. This study aimed to identify functional cell membrane proteins that promote HCC tumor initiation.

Experimental Procedures

Cell lines and culture

Human HCC cell line PLC/PRF/5 and human embryonic kidney cell line HEK-293FT were obtained from American Type Culture Collection (ATCC) and cultured in Dulbecco's Modified Eagle Medium-high glucose (DMEM-HG) (Gibco, USA) supplemented with 10% (v/v) fetal bovine serum (FBS) (Gibco, USA) and 1× (50 unit/ml) penicillin-streptomycin cocktail (P/S) (Gibco, USA). Metastatic human HCC cell line MHCC-97L was obtained from Prof. Z.Y. Tang at Fudan University, Shanghai, and cultured in DMEM-HG with 10% FBS, 1× P/S, and 1 mM sodium pyruvate (NaPy). MHCC-97L cells were authenticated to have no contamination (see STR results in Supp. Fig. 1, http://links.lww.com/HEP/H887). All cells were sustained in a humidified incubator at 37°C with 5% CO_2. Confluent cells on the culture plate were passaged routinely by trypsinization using TrypLE™ Express Enzyme (Gibco, USA).

siRNA library screening for sphere formation

We used the Dharmacon Cherry-pick ON-Targetplus custom-made siRNA library for functional screening. Each candidate gene was targeted by a mixture of 4 siRNAs (SMARTpool format) of known siRNA sequences. The siRNA from the library was prepared according to manufacturer's instructions. Before transfecting the siRNA, PLC/PRF/5 and MHCC-97L cells were seeded in a 96-well plate at 2,500 and 5,000 cells per well, respectively, overnight. To transfect the cells, lipofectamine2000 transfection mixture with the siRNA was incubated at room temperature for 15-20 min according to manufacturer's instruction before addition to the wells with the seeded cells. Upon 48 hours after transfecting the siRNAs, the cells were trypsinized by TrypLE™ Express Enzyme (Gibco, USA) for sphere formation assays.

Detailed experimental procedures for experiments in this study, including the lists of oligos for cloning shRNA constructs (Supp. Table 1, http://links.lww.com/HEP/H887), LANCL1 truncated mutants (Supp. Table 2, http://links.lww.com/HEP/H887), LANCL1 GSH-binding defective mutants (Supp. Table 3, http://links.lww.com/HEP/H887), LANCL1 mutants with Flag-tag (Supp. Table 4, http://links.lww.com/HEP/H887), LANCL1 mutants with deletion or mutations in 100^{th}-150^{th} aa region (Supp. Table 5, http://links.lww.com/HEP/H887), shRNA-resistant mutants of the indicated genes (Supp. Table 6, http://links.lww.com/HEP/H887), real-time quantitative PCR (qPCR) primer sequences (Supp. Table 7, http://links.lww.com/HEP/H887) and primary antibodies used (Supp. Table 8, http://links.lww.com/HEP/H887), are provided in the Supplementary Material.

Results

Discovery of LANCL1 as a potential cell surface protein responsible for liver tumor initiation.

We first compiled a comprehensive gene list based on the cluster of differentiation family genes (defined by HUGO Nomenclature Committee) and the Gene Ontology term “intrinsic component of plasma membrane” (GO:0031226). The list comprised all annotated genes related to cellular membranes. We then derived the differential expression data from both TCGA (50 pairs of tumor [T]/non-tumorous liver [NTL]) and our in-house (41 T/NTL pairs) RNA-sequencing (RNA-seq) datasets. With a false discovery rate <0.05, a list of 134 genes with expression of log2(T/NTL) >1 was identified as membrane-related genes upregulated in HCC than corresponding NTLs (Supp. Table 9, http://links.lww.com/HEP/H887).

We further interrogated the shortlisted genes using a customized siRNA library for functional screening (please refer to the details described in the Materials and Methods) (**Fig. 1A)**. Upon siRNA transfection in two HCC cell lines, PLC/PRF/5 and MHCC-97L (both are HBV-integrated HCC cells with spheroid-forming capability), we subjected the cells to sphere formation assay. With a criterion of ≥2-fold suppression of sphere formation by the siRNA as compared to the non-target control (NTC) in both cell lines in ≥ 3 of 5 trials, we identified 19 candidates (Supp. Table 9, http://links.lww.com/HEP/H887). Knockdown (KD) efficiency was validated by real-time quantitative PCR (qPCR) We chose candidates that were not well characterized in HCC (Supp. Table 10) and further validated the result with stable KD of the gene candidates (Supp. Fig. 2A-2B, http://links.lww.com/HEP/H887). By examining for any membrane staining pattern in immunofluorescence (IF) for the Flag-tagged candidate proteins, we identified four targets having a membranous pattern (Supp. Fig. 2C-2H, http://links.lww.com/HEP/H887). Finally, supported by the suppressive effects of KD on tumor-initiating ability in vivo in male NOD-SCID mice (Supp. Fig. 2I, http://links.lww.com/HEP/H887), Lanthionine synthase C-like protein 1 (LANCL1) was considered to be a promising target for further functional characterization. The whole screening process is summarized in **Fig. 1A**.

LANCL1 is an integral membrane protein.

The transmembranous regions on the cell membrane of the LANCL1 protein has not been well reported and this information has implications for therapeutic targeting. Here, we investigated the orientation of LANCL1 in the cell membrane by expressing both N-terminal and C-terminal Flag-tagged LANCL1 (**Fig. 1B**) in PLC/PRF/5 cells and examining them with IF using

anti-Flag antibody with or without cell membrane permeabilization by triton X-100 (**Fig. 1B-1C**). N-terminal Flag-tagged LANCL1 was detectable irrespective of the use of membrane permeabilization, indicating its extracellular localization (**Fig. 1C**). In contrast, C-terminal Flag-tagged LANCL1 was only detectable upon membrane permeabilization, indicating its intracellular localization (**Fig. 1C**). To delineate the exact structural location of LANCL1 protein transmembrane region, we expressed the various LANCL1 proteins with insertion of Flag-tag at different positions (**Fig. 1B**) in PLC/PRF/5 cells for immunofluorescence (IF), with or without cell membrane permeabilization (**Fig. 1C**). Like the N-terminal Flag-tagged protein, LANCL1 with Flag-tag inserted at the 50th and 100th aa-position showed membrane localization irrespective of membrane permeabilization (**Fig. 1C**). On the contrary, like the C-terminal Flag-tagged protein, those Flag-tags inserted at the 150th and 200th aa-positions were detected only upon membrane permeabilization, indicating that the localization of transmembrane region is between 100th and 150th aa-positions.

In addition, the membranous pattern of LANCL1 localization in parental PLC/PRF/5 cells was confirmed using antibody targeting the N-terminal region of the endogenous LANCL1 protein by IF on unpermeabilized cells (**Fig. 1D**). Furthermore, overexpression of wild-type (WT) LANCL1 in HCC cells led to a marked increase of cell surface LANCL1 protein as detected with flow cytometry (**Fig. 1E**), while stable KD showed the reverse effect (**Fig. 1F**).

After verifying LANCL1 as a transmembrane cell-surface protein, we further looked into the amino acid sequence between 100th and 150th aa to identify the exact transmembranous region of LANCL1 by corresponding experimental assays in HCC cells. In the Uniprot database, there

is prediction of α-helices for 111th-123rd aa, 127th-138th aa, and 139th-143rd aa. We therefore created respective deletion mutants of LANCL1 for the α-helices 111th-123rd aa and 127th-143rd aa, as well as the surrounding regions for 101st-110th aa and 144th-150th aa (Supp. Fig. 3A, http://links.lww.com/HEP/H887). On the other hand, there was report of conserved aa sequences of GXXG for LANCL1 protein across multiple species of organisms(9). These included the GDAG for 109th-112th aa of human LANCL1, and we questioned whether this specific sequence also played a role in the membrane localization of LANCL1 protein. We created a mutant with the two glycine (G) residues at 109th and 112th aa positions mutated into alanine (A) (G109A G112A mutant) (Supp. Fig. 3A, http://links.lww.com/HEP/H887). All these mutants were Flag-tagged at N-terminus and overexpressed in PLC/PRF/5 cells (Supp. Fig. 3B, http://links.lww.com/HEP/H887). Interestingly, upon permeabilization of the PLC/PRF/5 cells, all the mutants, except the 101st-110th aa-deleted and the G109A G112A mutants, showed membranous localization pattern as detected with IF using anti-Flag antibodies that target the extracellular N-terminal Flag tag (Supp. Fig. 3C, upper panel, http://links.lww.com/HEP/H887). The two exceptional mutants showed a diffuse cytoplasmic distribution. For the unpermeabilized cells, all the mutants, except the 101st-110th aa-deleted and the G109A G112A mutants and the WT LANCL1 with C-terminal intracellular Flag tag, showed membranous localization pattern (Supp. Fig. 3C, lower panel, http://links.lww.com/HEP/H887). These indicate that the two exceptional mutants failed to localize at the cell membrane to expose the N-terminal Flag tag extracellularly, implicating 101st-110th aa region as the key transmembrane domain to allow LANCL1 protein membrane localization.

LANCL1 promotes tumor initiation properties.

To validate the functional roles of LANCL1 in exerting tumor initiation properties, including sphere formation, in vivo tumorigenicity and chemoresistance, we established the LANCL1-KD and LANCL1-rescue (LANCL1-KD cells overexpressing LANCL1 variant which is not targetable by shRNA but has the same amino-acid sequence as WT-LANCL1 protein) HCC cells (**Fig. 2A**) **(**List of shRNA-resistant sequences of the mutants in Supp. Table 11, http://links.lww.com/HEP/H887**).** LANCL1 KD significantly reduced sphere-forming ability, whereas LANCL1-rescue reversed the inhibitory effects (**Fig. 2B**). To evaluate the tumor initiation and self-renewal ability of cells to generate a complete tumor in immunodeficient mice(10), we performed limiting dilution tumorigenicity assay using subcutaneous xenograft model(3, 11). LANCL1 KD suppressed the tumorigenicity and significantly reduced the frequency of tumor initiating cells (TICs), whereas LANCL1-rescue reversed the inhibitory effects (**Fig. 2C-2D** and Supp. Fig. 4A-4B, http://links.lww.com/HEP/H887). As three-dimensional organoid formation is contributed by liver progenitor cells or liver TICs(12, 13), we employed HCC organoids and observed that stable LANCL1-KD (Supp. Fig. 4C, http://links.lww.com/HEP/H887) significantly suppressed the organoid-forming ability (Supp. Fig. 4D, http://links.lww.com/HEP/H887).

As chemoresistance is another key feature in tumor initiation process, we investigated the effects of LANCL1-KD in sensitizing HCC cells to chemotherapy drugs, cisplatin and 5-fluorouracil (5-FU). LANCL1-KD sensitized HCC cells (Supp. Fig. 4E-4F, http://links.lww.com/HEP/H887) to these two drugs with significantly increased apoptosis. Furthermore, LANCL1-KD reduced the expression of various stemness-related gene (CD24, Nanog, Oct4, and Sox2) (Supp. Fig. 4G-4H, http://links.lww.com/HEP/H887).

LANCL1 suppresses reactive oxygen species (ROS) in HCC.

We next investigated whether LANCL1 suppressed intracellular ROS to promote sphere formation and tumorigenicity. We found that LANCL1-KD in PLC/PRF/5 and MHCC-97L increased the ROS levels in both spheroids and xenograft tumors, whereas LANCL1-rescue reversed the results (**Fig. 3A-3B** and Supp. Fig. 5A-5B, http://links.lww.com/HEP/H887). We subjected the control, LANCL1-KD, and LANCL1-rescued PLC/PRF/5 cells to RNA-seq and gene set enrichment analysis (GSEA) (Supp. Fig. 5C-5D, http://links.lww.com/HEP/H887). ROS-responsive gene set (Hallmark Reactive Oxygen Species Pathways) showed significant enrichment and upregulation in the LANCL1-KD group, as compared with the control and corresponding LANCL1-rescue groups (Supp. Fig. 5C-5E, http://links.lww.com/HEP/H887), respectively. Taken together, these data showed a consistent negative correlation between LANCL1 expression and ROS levels together with ROS-responsive gene expression.

Previously we reported that antioxidants, N-acetylcysteine (NAC) and glutathione (GSH), significantly suppressed ROS levels in HCC cells and xenografts(14). Here, we found that these exogenous antioxidants rescued the sphere formation that was suppressed by LANCL1-KD (**Fig. 3C**), but without altering the LANCL1 protein expression (Supp. Fig. 6A, http://links.lww.com/HEP/H887). Interestingly, both these two antioxidants suppressed the ROS levels upregulated by LANCL1-KD in HCC spheroid cells (**Fig. 3C** and Supp. Fig. 6B, http://links.lww.com/HEP/H887). Furthermore, the ROS increase induced by an oxidizing agent, tert-Butyl hydroperoxide (TBHP), was abrogated by NAC and GSH (Supp. Fig. 6C-6D, http://links.lww.com/HEP/H887). Of note, antioxidants also restored tumorigenicity which was

suppressed by LANCL1-KD in both PLC/PRF/5 and MHCC-97L (**Fig. 3D**), and abrogated ROS level increase induced by LANCL1-KD in xenografts as compared with that of NTC (**Fig. 3E** and Supp. Fig. 6E, http://links.lww.com/HEP/H887).

The suppression of ROS by LANCL1 is independent of its binding to GSH.

LANCL1 is a glutathione-S-transferase and binds to reduced GSH before transferring it to conjugate to the other xenobiotic substrate(15). As GSH can quench ROS to prevent oxidative stress(16), we investigated whether the suppressive effects on ROS levels by LANCL1 were dependent on its GSH-binding ability. We constructed LANCL1 mutants defective in GSH-binding by mutating the amino acid residues K317A, C322A and R364A, which were reported to be involved in GSH-binding(17). We made use of the P2A-tag system for tagging the rescued LANCL1 WT or mutant proteins with C-terminal P2A tag and simultaneous expression of blasticidin resistance gene to permit selection of successful stable clone cells. As P2A tag is not naturally found in animal cells, the re-expressed proteins can be distinguished from the endogenous LANCL1 proteins and successful expression of the corresponding P2A-tagged proteins can be verified by the detection of P2A tag. Mutation of either single residue K317A or all three residues sufficiently abolished GSH-binding ability of LANCL1, as demonstrated by pull-down assays using GSH-conjugated beads (**Fig. 4A**). Interestingly, both GSH-binding-defective mutants and WT-LANCL1 restored sphere formation originally suppressed upon LANCL1-KD (**Fig. 4B**), indicating that GSH-binding activity of LANCL1 is dispensable for sphere formation. In addition, similar to LANCL1 WT, GSH-binding-defective mutants blocked ROS increase in HCC spheroid cells (**Fig. 4C-4D**).

FAM49B is a top functional downstream binding partner of LANCL1 to suppress ROS and promote tumor initiation.

To investigate mechanisms by which LANCL1 suppressed ROS to promote tumor initiation, we performed RNA-seq on LANCL1-KD and rescue stable clones, with NTC for comparison. Excluding LANCL1 itself, there were no protein-coding genes altered by >2 folds between LANCL1-KD and NTC cells (Supp. Fig. 7A-7B, http://links.lww.com/HEP/H887), suggesting a lack of specific transcriptionally regulated targets downstream of LANCL1 in HCC. We then used the proteomic approach to look for co-immunoprecipitated binding partners of Flag-tagged LANCL1 pulled down by anti-Flag antibody in PLC/PRF/5 lysate and this revealed specific bands in the silver-stained image (Supp. Fig. 7C, http://links.lww.com/HEP/H887). On the other hand, by mass spectrometry, 20 potential targets were identified (**Fig. 5A**, upper panel). As LANCL1 is a membrane protein without nuclear expression, those targets with only nuclear expression (based on Human Protein Atlas database) were excluded, leaving 13 potential targets. Among the top hits, FAM49B, ADSL, ALDH16A1 and HSD17B10 were reported to be associated with ROS biology(18-21). Of note, FAM49B has been reported to suppress ROS generation in pancreatic ductal adenocarcinoma(21) and exert an oncogenic function in breast cancer(22). Functional screening by stable KD approach for all these potential targets in PLC/PRF/5 revealed that only FAM49B promoted sphere formation of HCC cells (Supp. Fig. 7D-7E, http://links.lww.com/HEP/H887). Moreover, FAM49B-KD increased ROS levels in HCC cells (Supp. Fig. 7F-7G, http://links.lww.com/HEP/H887), in line with the functional effects of LANCL1. Further, we confirmed with co-immunoprecipitation (Co-IP) the physical binding between FAM49B and LANCL1 (**Fig. 5A**, lower panel).

We further delineated the relationship between LANCL1 and FAM49B by overexpressing FAM49B in LANCL1-KD cells and LANCL1 in FAM49B-KD cells. Stable FAM49B overexpression restored the sphere formation of LANCL1-KD cells and abrogated ROS increase induced by LANCL1-KD in PLC/PRF/5 spheroid cells (**Fig. 5B** and Supp. Fig. 7H, http://links.lww.com/HEP/H887). Similarly, it restored tumor initiation (**Fig. 5C** and Supp. Fig. 7I) and suppressed back the ROS increase in the xenograft tumor cells (**Fig. 5C** and Supp. Fig. 7J, http://links.lww.com/HEP/H887). However, LANCL1 overexpression in FAM49B-KD cells failed to restore sphere formation (Supp. Fig. 8A, http://links.lww.com/HEP/H887) and abrogate the FAM49B-KD-induced ROS increase (Supp. Fig. 8B, http://links.lww.com/HEP/H887), indicating FAM49B is the key downstream binding partner to drive LANCL1-induced ROS reduction and functional effects.

LANCL1-FAM49B axis suppresses Rac1/NOX-driven intracellular ROS.

FAM49B inhibits the activation of Rac1, a small GTP-binding GTPase(23). Rac1 activation promotes ROS production by NADPH oxidases (NOXs)(24). Therefore, we asked whether upregulation of the LANCL1-FAM49B axis would suppress Rac1 activation to reduce ROS. Indeed, either LANCL1-KD or FAM49B-KD upregulated the level of activated Rac1 protein that specifically bound to PAK-PBD beads in Rac1-GTP pull-down assays (**Fig. 5D** and Supp. Fig. 8C, http://links.lww.com/HEP/H887), and this enhancement was abolished upon FAM49B overexpression in LANCL1-KD cells (**Fig. 5D**).

Next, we used Rac1 inhibitor (NSC23766) and NOX inhibitor (VAS2870), respectively, to

verify the involvement of Rac1-NOX signaling in LANCL1-FAM49B axis-driven suppression of ROS. We found that both inhibitors abolish the LANCL1-KD- or FAM49B-KD-induced ROS increase (**Fig. 5E** and Supp. Fig. 8D, http://links.lww.com/HEP/H887). Interestingly, Rac1 inhibitor but not NOX inhibitor abolished the Rac1-GTP level increase driven by LANCL1-KD or FAM49B-KD (Supp. Fig. 8E, http://links.lww.com/HEP/H887), indicating that NOX inhibition cannot suppress Rac1 activation, and Rac1-driven NOX is likely the final downstream effector suppressed by LANCL1-FAM49B signaling to inhibit ROS production. Therefore, we further determined NOX activity by measuring NADP+/NADPH ratio upon LANCL1-KD or FAM49B-KD in HCC cells. We found that both LANCL1-KD and FAM49B-KD increased NADP+/NADPH ratio, which was reverted by NSC23766 and VAS2870 treatment (**Fig. 5F**). All these suggest LANCL1-FAM49B axis reduces oxidative stress by suppressing Rac1-NOX signaling in HCC.

LANCL1 stabilizes FAM49B protein by blocking TRIM21-driven FAM49B ubiquitination and proteasomal degradation.

LANCL1 KD reduced FAM49B protein level (Supp. Fig. 9A upper panel, http://links.lww.com/HEP/H887). This reduction was not due to reduction in FAM49B mRNA (Supp. Fig. 9A lower panel, http://links.lww.com/HEP/H887), as it was abolished by LANCL1-rescue and proteasome inhibitor MG132. We further interrogated FAM49B protein stability at serial time-points upon protein synthesis blockade with cycloheximide (CHX). We found that LANCL1-KD with 2 independent shRNAs reduced FAM49B protein stability as compared to NTC, with shortened degradation half-life, and this was reversed by LANCL1-rescue (**Fig. 6A** left panel and Supp. Fig. 9B, http://links.lww.com/HEP/H887).

Furthermore, the reduced protein stability was due to enhanced ubiquitination of FAM49B protein upon LANCL1-KD and this was abolished after LANCL1-rescue (**Fig. 6A** right panel).

LANCL1 is not a ubiquitin enzyme (E1, E2, E3) and hence likely engages specific ubiquitin enzymes to participate in ubiquitination of FAM49B protein. By scrutinizing our LANCL1 interactome mass spectrometry data, we noted two potential LANCL1-binding proteins (TRIM21 and PSME3) as ubiquitination regulator(25, 26). Further functional screening revealed KD of TRIM21, but not PSME3, led to increased sphere formation and reduced ROS in HCC spheroid cells (**Fig. 6B-6C** and Supp. Fig. 9C). Surprisingly, with Co-IP, we found that TRIM21 interacted not only with LANCL1 but also FAM49B protein in HCC cells (**Fig. 6D**). TRIM21-KD increased both LANCL1 and FAM49B protein amounts while TRIM21 overexpression showed the opposite results; interestingly, the changes in the amounts of the two proteins upon TRIM21 manipulation were abolished by MG132 (Supp. Fig. 9D, http://links.lww.com/HEP/H887). In fact, MG132 increased the basal levels of both LANCL1 and FAM49B proteins (Supp. Fig. 9D, http://links.lww.com/HEP/H887), and the enhancing effect of MG132 on FAM49B protein level was more pronounced when endogenous FAM49B protein level was low in the LANCL1-KD background (Supp. Fig. 9A, http://links.lww.com/HEP/H887). This prompted us to further discover that TRIM21-KD decreased LANCL1 and FAM49B degradation half-life upon protein synthesis inhibition by CHX (**Fig. 6E** left panel and Supp. Fig. 9E, http://links.lww.com/HEP/H887), while TRIM21 overexpression reversed the results (Supp. Fig. 9F-9G, http://links.lww.com/HEP/H887). By detecting ubiquitination in immunoprecipitated LANCL1 and FAM49B proteins, we found that TRIM21-KD and overexpression reduced and increased ubiquitination, respectively, of both

proteins (**Fig. 6E** right panel and Supp. Fig. 9H, http://links.lww.com/HEP/H887), indicating that both LANCL1 and FAM49B are protein substrates for ubiquitination by TRIM21. Next, we investigated the binding between FAM49B and TRIM21 upon LANCL1-KD and LANCL1-rescue by Co-IP, in which protein degradation blockade by MG132 ensured equal amounts of FAM49B and TRIM21 protein input for fair comparison. We found enhanced TRIM21/FAM49B mutual binding upon LANCL1-KD and this was abolished when LANCL1 was rescued (**Fig. 6F**). These data indicate that TRIM21 participates in LANCL1-FAM49B-axis-mediated ROS regulation and functionality.

LANCL1 abrogates the inhibitory effects of TRIM21 on tumor initiation properties.

LANCL1 and FAM49B protein reduction by TRIM21 overexpression in PLC/PRF/5 cells was reversed by LANCL1 overexpression (**Fig. 7A**). LANCL1 upregulation restored sphere-forming ability and ROS downregulation, which were suppressed by TRIM21 overexpression (**Fig. 7B** and Supp. Fig. 10A, http://links.lww.com/HEP/H887). Similarly, TRIM21 upregulation suppressed tumorigenicity in vivo and increased ROS in xenograft tumor cells, both of which were abolished by LANCL1 overexpression (**Fig. 7C-7D** and Supp. Fig. 10B-10C, http://links.lww.com/HEP/H887).

The intracellular C-terminal region of LANCL1 is critical in promoting sphere formation.

LANCL1 is a membrane protein with an intracellular C-terminal domain. As we demonstrated , LANCL1 engaged two cytosolic proteins FAM49B and TRIM21 and inhibited their interaction. Therefore, we investigated if LANCL1 C-terminal domain was functionally responsible for such interaction. We overexpressed LANCL1 proteins with progressive C-terminal truncation

(LANCL1 Δ201-399 and LANCL1 Δ301-399) in LANCL1-KD cells (**Fig. 7E**, top left panel) and subjected the cells to sphere formation and ROS assays. Overexpression of LANCL1 WT but not the C-terminal-truncated mutants reversed the suppressed sphere formation (**Fig. 7E,** top right and lower left panels) and ROS increase (**Fig. 7E** lower right panel and Supp. Fig. 10D, http://links.lww.com/HEP/H887) that were induced upon LANCL1-KD. Moreover, immunoprecipitation assays showed that C-terminal-truncated LANCL1 mutants failed to bind to FAM49B and TRIM21 proteins (**Fig. 7F**). The enhancement in the binding between TRIM21 and FAM49B proteins upon LANCL1-KD was abolished by overexpression of LANCL1 WT but not C-terminal-truncated LANCL1 (**Fig. 7F**). By detecting the ubiquitination of the immunoprecipitated FAM49B protein from stable clones of PLC/PRF/5 with rescue of LANCL1 WT or C-terminal truncated mutants (LANCL1 Δ201-399 and LANCL1 Δ301-399), respectively, upon LANCL KD, we found that the LANCL1 C-terminal truncated mutants failed to suppress ubiquitination of FAM49B while the LANCL1 WT did (Supp. Fig. 10E, http://links.lww.com/HEP/H887). We further performed cycloheximide assays to measure the FAM49B protein stability in the above stable clones and found that the rescue of LANCL1 C-terminal truncated-mutants (LANCL1 Δ201-399 and LANCL1 Δ301-399) failed to restore the reduced FAM49B protein stability **(**Supp. Fig.s 11B-C, 11E-F, http://links.lww.com/HEP/H887) upon LANCL1 KD while LANCL1 WT rescue could reverse the reduced FAM49B protein stability (Supp. Fig. 11A and 11D, http://links.lww.com/HEP/H887). All these implicate that LANCL1 C-terminal domain is essential in maintaining FAM49B protein stability by binding FAM49B and TRIM21 to inhibit the direct interaction between FAM49B and TRIM21 proteins.

High LANCL1 and FAM49B co-expression is associated with more advanced tumor stage, poorer overall survival and disease-free survival.

From the RNA-seq data in our in-house HKU-QMH (n=41 pairs) and TCGA-LIHC (n=50 pairs) cohorts, both LANCL1 and FAM49B were significantly overexpressed in HCC tumors as compared with the corresponding NTLs (P<0.0001) (Supp. Fig. 12A, http://links.lww.com/HEP/H887). In an independent cohort (n=98 pairs) of our HCCs, both were significantly upregulated by >2 folds in HCCs in around 50% of the cases (Supp. Fig. 12B, http://links.lww.com/HEP/H887). The clinicopathological features of the patients with HCC are listed in Supp. Table 12, http://links.lww.com/HEP/H887. We found a significantly positive correlation between LANCL1 and FAM49B expression in HCCs (Supp. Fig. 12C, http://links.lww.com/HEP/H887). A previous study showed that FAM49B upregulation was associated with poorer prognosis in HCC patients(27). To this end, we analyzed the clinical significance of LANCL1 and FAM49B co-expression. We defined high and low LANCL1 or FAM49B expression by T/NTL >2 and T/NTL ≤2, respectively. We observed that the HCC subgroup with high co-expression of LANCL1 and FAM49B had more advanced tumor stage and poorer cellular differentiation **(Fig. 8A**), poorer overall and disease-free survival (**Fig. 8B** and Supp. Fig. 12D, http://links.lww.com/HEP/H887). Interestingly, the association with poorer overall and disease-free survival was not observed with LANCL1 by itself (Supp. Fig. 12E, http://links.lww.com/HEP/H887). This highlights our aforementioned findings that LANCL1 is a critical determinant for FAM49B expression, upregulation of LANCL1 enhanced the role of FAM49B in association with more aggressive tumor behavior and poorer prognosis of HCC.

Anti-LANCL1 antibodies against the extracellular N-terminal region suppress the sphere

forming ability of HCC cells.

We further tested the translational potential of blocking cell-surface LANCL1 with antibodies against the extracellular N-terminal region of LANCL1. These include the antibodies generated against the N-terminal 1-47aa region of LANCL1 as immunogen for NBP1-81796 (Novus Biological, USA) and HPA034994 (Sigma-Aldrich, St. Louis), and the N-terminal 1-58aa region for H00010314-A01 (Abnova, Taiwan). We found that the blocking antibodies significantly suppressed sphere formation of PLC/PRF/5 cells as compared to the respective IgG controls (**Fig. 8C** and Supp. Fig. 13A-13B, http://links.lww.com/HEP/H887).

Discussion

Liver tumor initiation was contributed by several specific functional cell-surface proteins (CD24, CD47, CD90, CD133, etc.) that not only initiate HCC, but also promote HCC recurrence, drug resistance, and adverse prognosis(28, 29). Targeting the surface protein responsible for tumor initiation is one of the most important strategies in cancer treatment(30). Here, we searched for novel cell surface protein driving tumor initiation by using tailor-made siRNA library with sphere formation ability as a readout in HCC cells. Upon validation of membranous localization and subsequent functional verification, we identified LANCL1 as a potential functional cell surface protein for further comprehensive study.

It was reported that an efficient ROS-scavenging system by increased transfer of GSH is important for LANCL1-mediated tumor initiation (31) and survival of prostate cancer cells (32) or neuronal cells(15) under oxidative stress condition. We found that LANCL1 reduced the

cellular ROS levels to promote the tumor initiation properties of HCC cells. Unexpectedly, LANCL1-driven ROS suppression was independent of GSH, as exemplified by the ability of antioxidant GSH to abrogate ROS increase even in LANCL1-KD cells. By creating LANCL1 mutants with mutated GSH-binding sites of LANCL1, we also found that the positive roles of LANCL1 on ROS suppression and promotion of tumor initiation were independent of GSH-binding ability. These unexpected results implicate that LANCL1 does not function as a GSH-transferase in relation to enhancement of tumor initiation properties. ROS has been reported to promote cell death and inhibit pro-tumorigenic properties like multi-drug resistance of HCC cells (33) and by altering multiple cell signaling pathways (14, 34, 35), indicating a negative role of ROS in tumor growth. Nevertheless, cancer cells employ multiple ways to counteract the anti-proliferative ROS and resulting oxidative stress, including nuclear erythroid 2-related factor 2 (Nrf2) stabilization (36) to drive expression of downstream antioxidant effectors (14), to mediate protection against oxidative stress.

In this study, our findings suggested a novel mechanism of how LANCL1 downregulates ROS levels to promote tumor initiation (**Fig. 8D**). We demonstrated that FAM49B is a top functional downstream binding partner of LANCL1 to suppress ROS and promote tumor initiation. We further found that TRIM21 was the sole ubiquitin ligase with binding ability to LANCL1 and FAM49B to exert a functional phenotypic outcome in terms of suppression of tumor initiation properties. LANCL1 enhances FAM49B protein level by interfering the interaction between FAM49B and TRIM21, thereby protecting FAM49B protein from proteasomal degradation process induced by TRIM21. Enrichment of FAM49B protein inhibits Rac1 activation, which in turn reduces NOX-mediated ROS production. Altogether, this

TRIM21-LANCL1-FAM49B-Rac1-NOXs-ROS signaling axis promotes liver tumor initiation. As PLC/PRF/5 and MHCC-97L have low expression of typical liver TIC markers like CD133 and EpCAM, our study has pinpointed the above LANCL1-related signaling pathway as a novel alternative pathway that contributes to the tumor initiation in a CD133- or EpCAM-independent manner.

Although TRIM21 has been suggested to have an oncogenic role (37), there are recent publications that support the opposite. For instance, TRIM21 downregulation in liver cancer samples was associated with advanced tumor stage and poorer prognosis (38). TRIM21 also promotes the ubiquitination of β-catenin and suppresses PI3K-Akt pathways in HCC cells (39), suppressing multiple pro-tumorigenic signaling pathways. The above contradictory findings may reflect the context-dependent nature of the functional roles of TRIM21 in HCC initiation. Analyzing the survival rates for high LANCL1 or high FAM49B expression in patient subgroups having different TRIM21 expression (Supp. Fig. 14A-D, http://links.lww.com/HEP/H887), we found that high FAM49B expression was associated with poorer overall survival of HCC patients of low TRIM21 subgroup (Supp. Fig. 14B right panel, http://links.lww.com/HEP/H887), implicating potentially more stable protein expression of FAM49B with low TRIM21 background.

To allow clinical translation of LANCL1-targeting therapy, we researched the cell surface protein domain of LANCL1 and verified LANCL1 as an integral membrane protein with extracellular N-terminal, intracellular C-terminal, and transmembrane region mapped at

101st-110th aa, which have never been reported before. A previous study on the in vitro LANCL1 protein crystal structure showed the involvement of R4, K317, C322, and R364 amino acid residues in proximity for GSH-binding(17). However, we found that the R4 residue should be extracellular and unable to interact with the other three intracellular residues. By progressive C-terminal truncation method, we demonstrated that LANCL1 intracellular C-terminal domain is functional, stabilizing FAM49B protein to exert its downstream effects in HCC. Intriguingly, using multiple antibodies designed to target the extracellular N-terminal domain of LANCL1 protein, we found that blocking cell-surface LANCL1 could significantly suppress sphere formation.

Looking forward, targeting LANCL1-FAM49B axis may be a promising strategy for HCC treatment. However, there are several issues that warrant further investigation. First, the identification of specific functional ligands of LANCL1 in HCC cells will allow blockade of LANCL1-ligand binding. Second, LANCL1 antibodies with better affinity against the LANCL1 N-terminal region on unfixed live cells are needed to allow therapeutic application. Third, since LANCL1 protein expression is not specific to HCC cells, we may need to address the specificity issue of LANCL1-targeting strategies or delivery of LANCL1-targeting antibodies. Fourth, the functional and molecular linkage between the extracellular N-terminal and intracellular C-terminal domains of the LANCL1 protein is still not yet clear but beyond the scope of our current study. Therefore, further study on whether and how the blockade of extracellular domain of LANCL1 will affect the interaction of its C-terminal domain with the FAM49B/TRIM21 complex is worthy.

References

1. Zhou BB, Zhang H, Damelin M, Geles KG, Grindley JC, Dirks PB. Tumor-initiating cells: challenges and opportunities for anticancer drug discovery. Net Rev Drug Discov. 2009;8(10):806-23.
2. Haraguchi N, Ishii H, Mimori K, Tanaka F, Ohkuma M, Kim HM, et al. CD13 is a therapeutic target in human liver cancer stem cells. J Clin Invest. 2010;120(9):3326-39.
3. Lee TK, Castilho A, Cheung VC, Tang KH, Ma S, Ng IO. CD24(+) liver tumor-initiating cells drive self-renewal and tumor initiation through STAT3-mediated NANOG regulation. Cell Stem Cell. 2011;9(1):50-63.
4. Lee TK, Cheung VC, Lu P, Lau EY, Ma S, Tang KH, et al. Blockade of CD47-mediated cathepsin S/protease-activated receptor 2 signaling provides a therapeutic target for hepatocellular carcinoma. Hepatology. 2014;60(1):179-91.
5. Yang ZF, Ho DW, Ng MN, Lau CK, Yu WC, Ngai P, et al. Significance of CD90+ cancer stem cells in human liver cancer. Cancer Cell. 2008;13(2):153-66.
6. Ma S, Chan KW, Hu L, Lee TK, Wo JY, Ng IO, et al. Identification and characterization of tumorigenic liver cancer stem/progenitor cells. Gastroenterology. 2007;132(7):2542-56.
7. Yamashita T, Ji J, Budhu A, Forgues M, Yang W, Wang HY, et al. EpCAM-positive hepatocellular carcinoma cells are tumor-initiating cells with stem/progenitor cell features. Gastroenterology. 2009;136(3):1012-24.
8. Yamashita T, Honda M, Nakamoto Y, Baba M, Nio K, Hara Y, et al. Discrete nature of EpCAM+ and CD90+ cancer stem cells in human hepatocellular carcinoma. Hepatology. 2013;57(4):1484-97.
9. Bauer, H., Mayer, H., Marchler-Bauer, A., Salzer, U. and Prohaska, R. Characterization of p40/GPR69A as a peripheral membrane protein related to the lantibiotic synthetase component C. Biochem Biophys Res Commun. 2000;275(1):69–74.
10. Tirino V, Desiderio V, Paino F, De Rosa A, Papaccio F, La Noce M, et al. Cancer stem cells in solid tumors: an overview and new approaches for their isolation and characterization. FASEB J. 2013;27(1):13-24.
11. Cui CP, Wong CC, Kai AK, Ho DW, Lau EY, Tsui YM, et al. SENP1 promotes hypoxia-induced cancer stemness by HIF-1alpha deSUMOylation and SENP1/HIF-1alpha positive feedback loop. Gut. 2017;66(12):2149-59.
12. Broutier L, Mastrogiovanni G, Verstegen MM, Francies HE, Gavarro LM, Bradshaw CR, et al. Human primary liver cancer-derived organoid cultures for disease modeling and drug screening. Nat Med. 2017;23(12):1424-35.

13. Huch M, Gehart H, van Boxtel R, Hamer K, Blokzijl F, Verstegen MM, et al. Long-term culture of genome-stable bipotent stem cells from adult human liver. Cell. 2015;160(1-2):299-312.
14. Zhang VX, Sze KM, Chan LK, Ho DW, Tsui YM, Chiu YT, et al. Antioxidant supplements promote tumor formation and growth and confer drug resistance in hepatocellular carcinoma by reducing intracellular ROS and induction of TMBIM1. Cell Biosci. 2021;11(1):217.
15. Huang C, Chen M, Pang D, Bi D, Zou Y, Xia X, et al. Developmental and activity-dependent expression of LanCL1 confers antioxidant activity required for neuronal survival. Dev Cell. 2014;30(4):479-87.
16. Mailloux RJ, McBride SL, Harper ME. Unearthing the secrets of mitochondrial ROS and glutathione in bioenergetics. Trends Biochem Sci. 2013;38(12):592-602.
17. Zhang W, Wang L, Liu Y, Xu J, Zhu G, Cang H, et al. Structure of human lanthionine synthetase C-like protein 1 and its interaction with Eps8 and glutathione. Genes Dev. 2009;23(12):1387-92.
18. Taha-Mehlitz S, Bianco G, Coto-Llerena M, Kancherla V, Bantug GR, Gallon J, et al. Adenylosuccinate lyase is oncogenic in colorectal cancer by causing mitochondrial dysfunction and independent activation of NRF2 and mTOR-MYC-axis. Theranostics. 2021;11(9):4011-29.
19. Vasiliou V, Thompson DC, Smith C, Fujita M, Chen Y. Aldehyde dehydrogenases: from eye crystallins to metabolic disease and cancer stem cells. Chem Biol Interact. 2013;202(1-3):2-10.
20. Vinklarova L, Schmidt M, Benek O, Kuca K, Gunn-Moore F, Musilek K. Friend or enemy? Review of 17beta-HSD10 and its role in human health or disease. J Neurochem. 2020;155(3):231-49.
21. Chattaragada MS, Riganti C, Sassoe M, Principe M, Santamorena MM, Roux C, et al. FAM49B, a novel regulator of mitochondrial function and integrity that suppresses tumor metastasis. Oncogene. 2018;37(6):697-709.
22. **Li, Y., Xiong, Y.**, Wang, Z., Han, J., Shi, S., He, J., et el. FAM49B promotes breast cancer proliferation, metastasis, and chemoresistance by stabilizing ELAVL1 protein and regulating downstream Rab10/TLR4 pathway. Cancer cell international. 2021;21(1):534.
23. **Yuki KE, Marei H, Fiskin E, Eva MM**, Gopal AA, Schwartzentruber JA, et al. CYRI/FAM49B negatively regulates RAC1-driven cytoskeletal remodelling and protects against bacterial infection. Nat Microbiol. 2019;4(9):1516-31.
24. Cheng G, Diebold BA, Hughes Y, Lambeth JD. Nox1-dependent reactive oxygen generation is regulated by Rac1. J Biol Chem. 2006;281(26):17718-26.
25. Sun J, Luan Y, Xiang D, Tan X, Chen H, Deng Q, et al. The 11S Proteasome Subunit PSME3 Is a Positive Feedforward Regulator of NF-kappaB and Important for Host Defense

against Bacterial Pathogens. Cell Rep. 2016;14(4):737-49.
26. Fletcher AJ, Mallery DL, Watkinson RE, Dickson CF, James LC. Sequential ubiquitination and deubiquitination enzymes synchronize the dual sensor and effector functions of TRIM21. Proc Natl Acad Sci U S A. 2015;112(32):10014-9.
27. Xu F, Chen J, Huang D. Pan-cancer analysis identifies FAM49B as an immune-related prognostic maker for hepatocellular carcinoma. J Cancer. 2022;13(1):278-89.
28. **Tsui YM, Chan LK,** Ng IO. Cancer stemness in hepatocellular carcinoma: mechanisms and translational potential. Br J Cancer. 2020;122(10):1428-40.
29. Agliano A, Calvo A, Box C. The challenge of targeting cancer stem cells to halt metastasis. Semin Cancer Biol. 2017;44:25-42.
30. Tovar V, Cornella H, Moeini A, Vidal S, Hoshida Y, Sia D, et al. Tumour initiating cells and IGF/FGF signalling contribute to sorafenib resistance in hepatocellular carcinoma. Gut. 2017;66(3):530-40.
31. Diehn M, Cho RW, Lobo NA, Kalisky T, Dorie MJ, Kulp AN, et al. Association of reactive oxygen species levels and radioresistance in cancer stem cells. Nature. 2009;458(7239):780-
32. Wang J, Xiao Q, Chen X, Tong S, Sun J, Lv R, et al. LanCL1 protects prostate cancer cells from oxidative stress via suppression of JNK pathway. Cell Death Dis. 2018;9(2):197.
33. Perillo B, Di Donato M, Pezone, A., Di Zazzo, E., Giovannelli, P., Galasso, G., et al. ROS in cancer therapy: the bright side of the moon. Exp Mol Med. 2020;52(2):192–203.
34. Lv X, Yu H, Zhang Q., Huang, Q., Hong, X., Yu, T., et al. SRXN1 stimulates hepatocellular carcinoma tumorigenesis and metastasis through modulating ROS/p65/BTG2 signalling. J Cell Mol Med. 2020;24(18):10714–10729.
35. Chiba T, Suzuki E, Yuki K, Zen Y, Oshima M, Miyagi S, et al. Disulfiram eradicates tumor-initiating hepatocellular carcinoma cells in ROS-p38 MAPK pathway-dependent and -independent manners. PloS one. 2014;9(1):e84807.
36. Kovac S, Angelova PR, Holmström KM, Zhang Y, Dinkova-Kostova AT, Abramov AY. Nrf2 regulates ROS production by mitochondria and NADPH oxidase. Biochimica et Biophysica Acta 2015;1850(4):794–801.
37. Wang F, Zhang Y, Shen J, Yang B, Dai W, Yan J, et al. The Ubiquitin E3 Ligase TRIM21 Promotes Hepatocarcinogenesis by Suppressing the p62-Keap1-Nrf2 Antioxidant Pathway. Cell Mol Gastroenterol Hepatol 2021;11(5):1369–1385.
38. Ding Q, He D, He K, Zhang Q, Tang M, Dai J, et al. Downregulation of TRIM21 contributes to hepatocellular carcinoma carcinogenesis and indicates poor prognosis of cancers. Tumour Biol. 2015;36(11):8761–8772.
39. Zhang Z, Zhu Z, Sheng H, Sun J, Cao C. TRIM21 suppresses invasion of hepatocellular

carcinoma cells by promoting β-catenin ubiquitylation and degradation. J Southern Med U. 2022;42(1):55–62.

ACKNOWLEDGEMENT

We thank the Centre for PanorOmic Sciences (CPOS) of the LKS Faculty of Medicine of the University of Hong Kong for providing the facilities and services for flow cytometry, mass spectrometry, and transcriptome analyses. We also thank Ms. Joyce Man-Fong for technical assistance and Dr. Abdullah Husain and Dr. Chen Ao for assistance in mouse work. We thank Dr. Meritxell Huch for HCC organoid.

Conflict of Interest

The authors have no conflict of interest.

Figure 1. LANCL1 is a potential functioning surface protein to drive tumor initiation in HCC. A. Screening strategy to find novel surface proteins that promote tumor initiation. B-C. Wild-type (WT) and mutants of LANCL1 with insertion of Flag-tag at different positions were expressed in PLC/PRF/5 cells (B), with expression location determined by immunofluorescence (C) using anti-Flag antibody (green) under permeabilizing (upper panel) and non-permeabilizing (lower panel) conditions. D. Immunofluorescence for non-permeabilized parental PLC/PRF/5 cells using anti-LANCL1 antibody (green). E-F. Flow cytometry to measure cell surface LANCL1 expression in LANCL1-overexpressing (C) or -KD (F) PLC/PRF/5 cells using anti-LANCL1 antibody targeting 1-47aa epitope. **p<0.01; Scale bar=10μm.

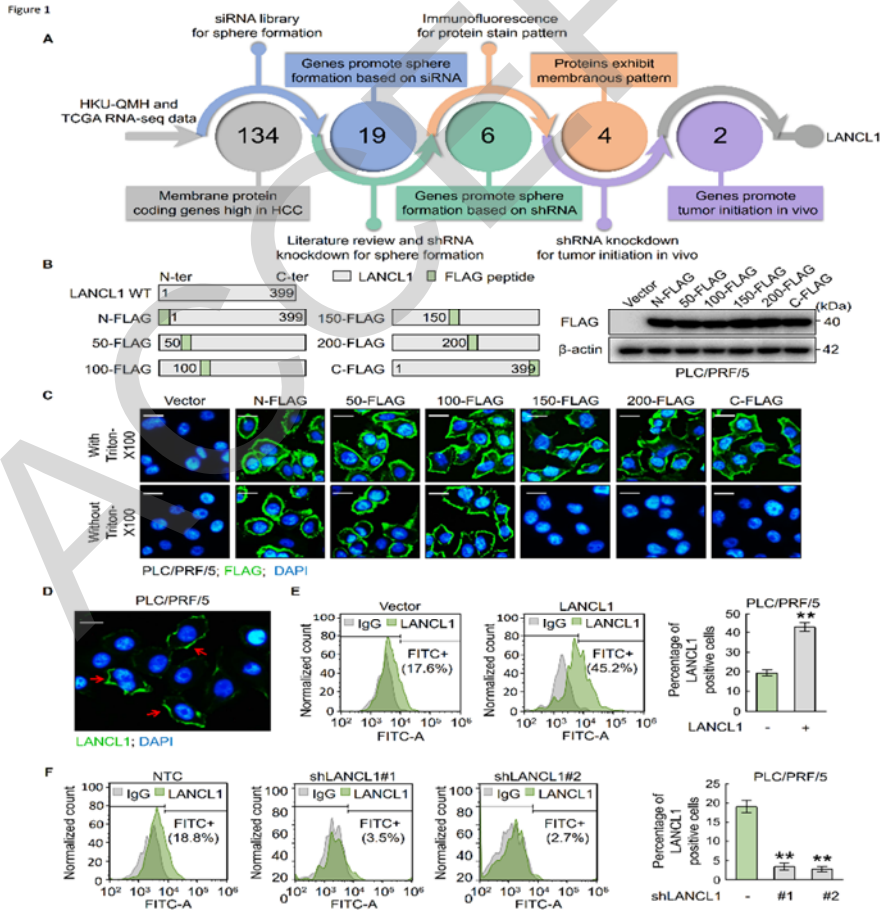

Figure 2. Knockdown of LANCL1 suppresses sphere formation ability which is reversed by protein rescue in HCC cells. A. Rescue of shRNA-resisted variant of LANCL1 in LANCL1-KD HCC cells. B. Sphere formation assays for the above-mentioned HCC cells. C-D. Limiting dilution assays in NOD-SCID mice with 5e5, 5e4, and 5e3 of the indicated PLC/PRF/5 (C) and MHCC-97L (D) cells subcutaneously injected. *p<0.05; **p<0.01; Scale bar=200μm.

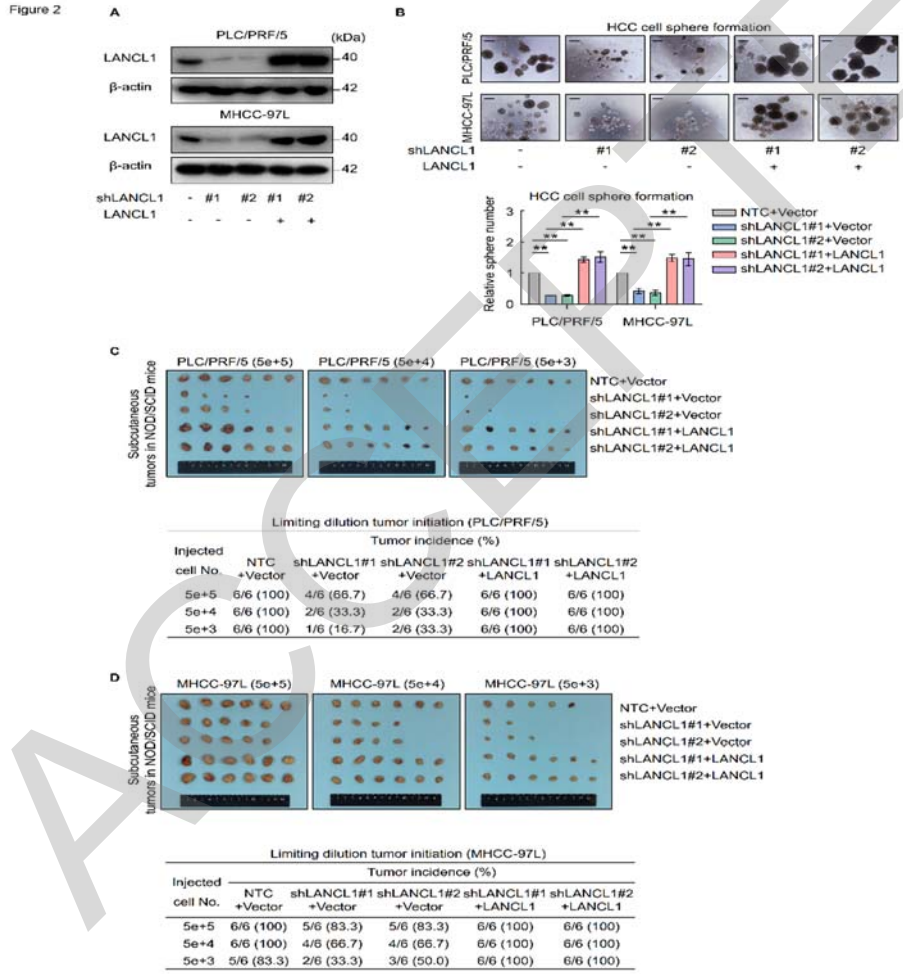

Limiting dilution tumor initiation (PLC/PRF/5)

Injected cell No.	Tumor incidence (%)				
	NTC +Vector	shLANCL1#1 +Vector	shLANCL1#2 +Vector	shLANCL1#1 +LANCL1	shLANCL1#2 +LANCL1
5e+5	6/6 (100)	4/6 (66.7)	4/6 (66.7)	6/6 (100)	6/6 (100)
5e+4	6/6 (100)	2/6 (33.3)	2/6 (33.3)	6/6 (100)	6/6 (100)
5e+3	6/6 (100)	1/6 (16.7)	2/6 (33.3)	6/6 (100)	6/6 (100)

Limiting dilution tumor initiation (MHCC-97L)

Injected cell No.	Tumor incidence (%)				
	NTC +Vector	shLANCL1#1 +Vector	shLANCL1#2 +Vector	shLANCL1#1 +LANCL1	shLANCL1#2 +LANCL1
5e+5	6/6 (100)	5/6 (83.3)	5/6 (83.3)	6/6 (100)	6/6 (100)
5e+4	6/6 (100)	4/6 (66.7)	4/6 (66.7)	6/6 (100)	6/6 (100)
5e+3	5/6 (83.3)	2/6 (33.3)	3/6 (50.0)	6/6 (100)	6/6 (100)

Figure 3. LANCL1 promotes tumor initiation by suppressing intracellular ROS levels.

A-B. ROS levels for PLC/PRF/5 and MHCC-97L spheroid cells (A) and xenograft tumor cells (B) of LANCL1-KD and LANCL1-rescue stable clones. C. LANCL1-KD HCC cells were treated with NAC (1 mM) or GSH (100 μM), or distilled water (Ctrl) for sphere formation assays. ROS levels were measured for HCC spheroid cells with treatment as mentioned (bottom). D-E. NOD-SCID mice with the indicated subcutaneous cell injection were fed with distilled water (Ctrl) or NAC (120 mg/kg/day), or GSH (100 mg/kg/day) for 4 weeks (top) to measure tumor incidence (bottom) and tumor cell ROS (E). *p<0.05; **p<0.01; Scale bar=200μm.

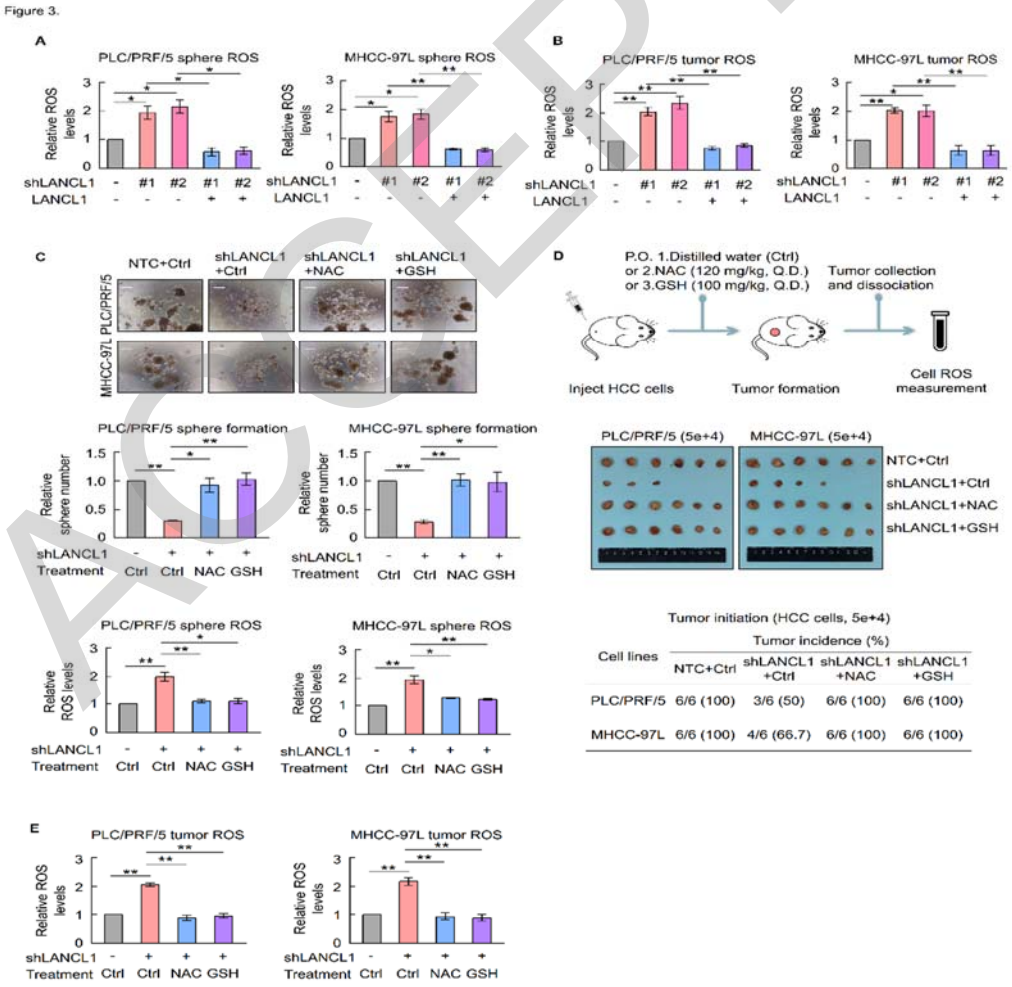

Tumor initiation (HCC cells, 5e+4)

Cell lines	Tumor incidence (%)			
	NTC+Ctrl	shLANCL1 +Ctrl	shLANCL1 +NAC	shLANCL1 +GSH
PLC/PRF/5	6/6 (100)	3/6 (50)	6/6 (100)	6/6 (100)
MHCC-97L	6/6 (100)	4/6 (66.7)	6/6 (100)	6/6 (100)

Figure 4. The suppression of ROS and sphere formation by LANCL1 is independent of its GSH-binding ability.

A. LANCL1-KD clones were rescued by LANCL1 WT or GSH-binding site mutants (K317A: LANCL1 K317A mutant, 3BS: LANCL1 K317A, C322A, and R364A mutant) in HCC cells. GSH-binding of the P2A-tagged LANCL1 WT and mutants was examined by pull-down using GSH-sepharose beads and immunoblotting. B-D. Sphere formation (B) and ROS (C-D) were examined. *p<0.05; **p<0.01; Scale bar=200μm.

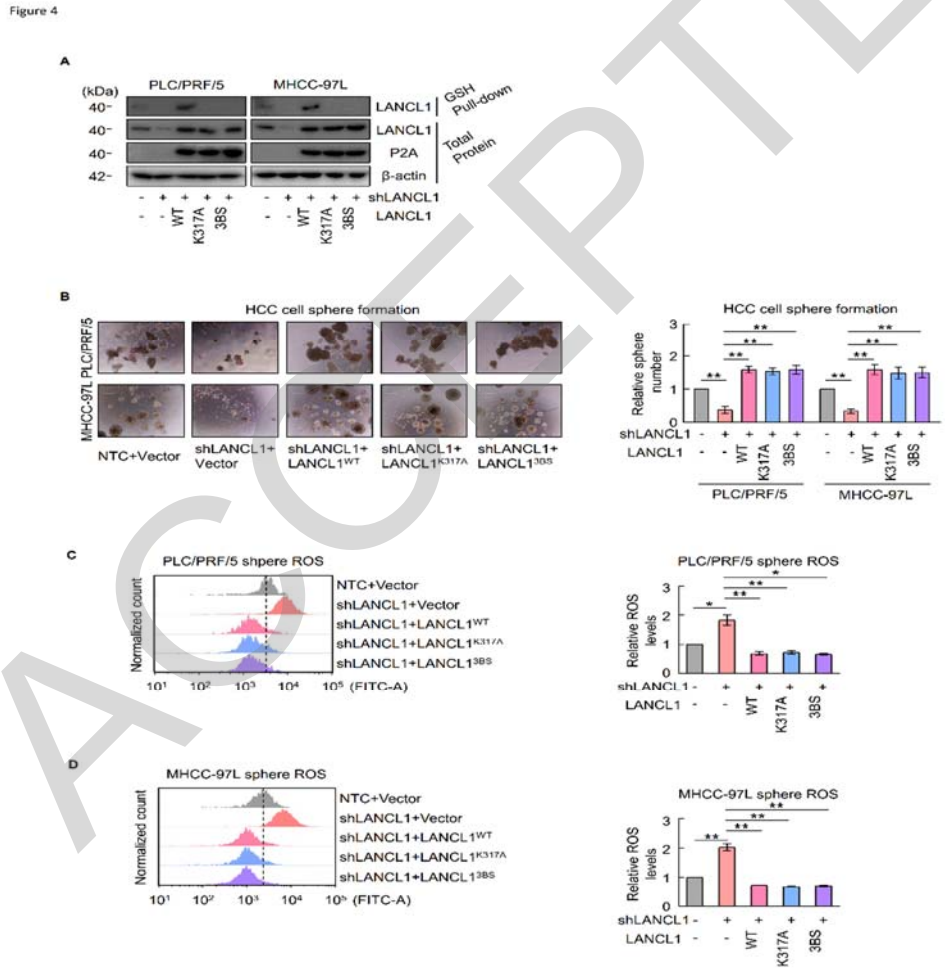

Figure 5. FAM49B is the downstream protein and reduces LANCL1-driven ROS via Rac1 inhibition and amelioration of NOX-mediated oxidative stress to promote tumor initiation-related properties. A. Proteins (red) significantly enriched by >4 folds in LANCL1 interactome in PLC/PRF/5 cells (upper). Endogenous FAM49B was co-immunoprecipitated with LANCL1 and vice versa (lower panels). B. Immunoblotting was performed for LANCL1-KD plus FAM49B-overexpression PLC/PRF/5 cells which also had the sphere formation and ROS level examined. C. Limiting dilution tumorigenicity assays for the above-mentioned PLC/PRF/5 cells. ROS level was examined for the indicated tumor cells. D. Rac1-GTP pull-down assays using PAK-PBD beads for the indicated PLC/PRF/5 cells with the indicated protein levels detected. E. ROS levels for the indicated PLC/PRF/5 cells with 24-hour treatment of NSC23766 (50 μM) and VAS2870 (10 μM). F. NADPH assays for the indicated PLC/PRF/5 cells with NSC23766 and VAS2870 treatment. NADP+ amount (pink) + NADPH amount (blue) = total NADP amount (NADPt) was indicated at left Y-axis. NADP+/NADPH ratio (grey) was indicated at right Y-axis. *p<0.05; **p<0.01; ns: not significant. Scale bar=200μm.

Figure 5

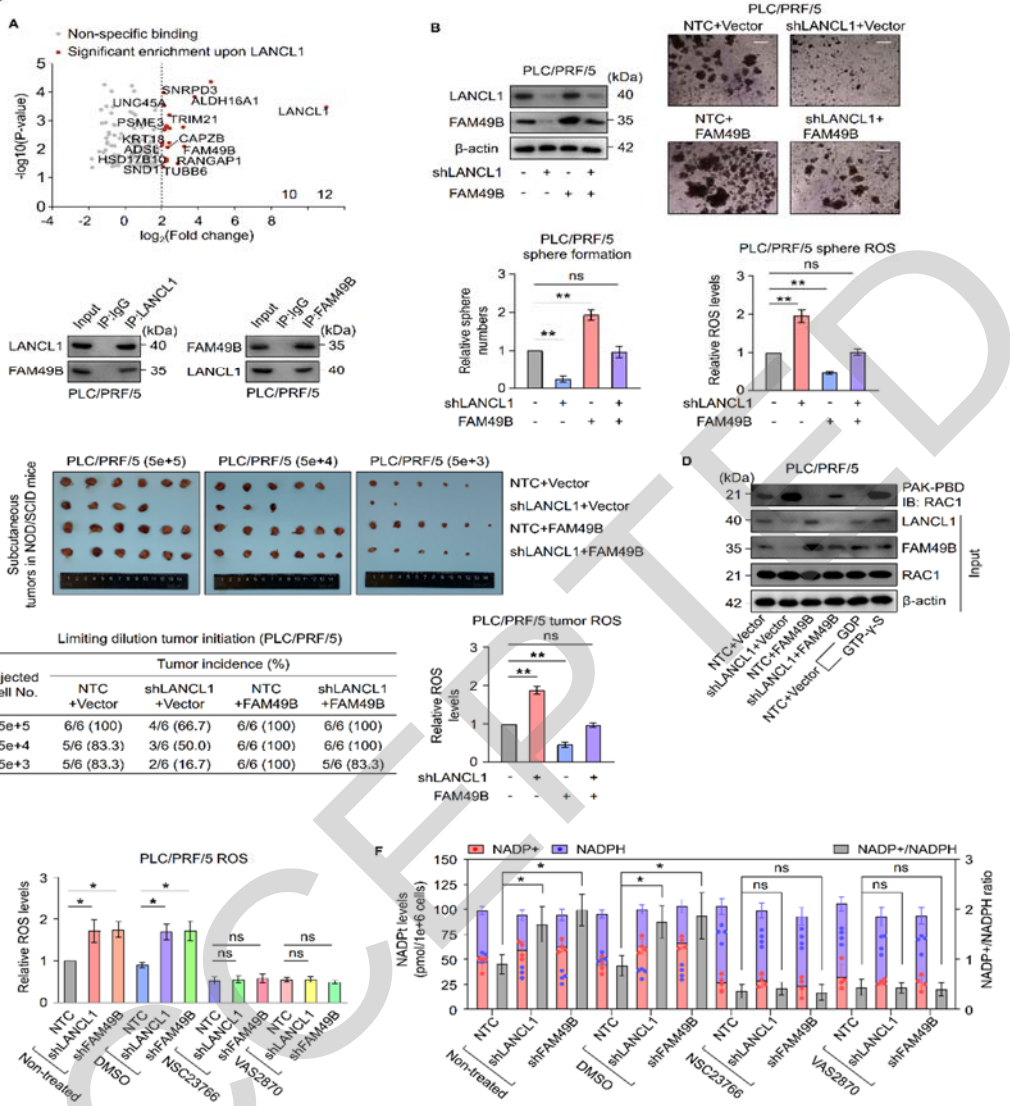

Limiting dilution tumor initiation (PLC/PRF/5)

Injected cell No.	Tumor incidence (%)			
	NTC +Vector	shLANCL1 +Vector	NTC +FAM49B	shLANCL1 +FAM49B
5e+5	6/6 (100)	4/6 (66.7)	6/6 (100)	6/6 (100)
5e+4	5/6 (83.3)	3/6 (50.0)	6/6 (100)	6/6 (100)
5e+3	5/6 (83.3)	2/6 (16.7)	6/6 (100)	5/6 (83.3)

Figure 6. LANCL1 blocks TRIM21 binding to FAM49B, reducing TRIM21-induced proteasomal degradation of FAM49B. A. Examination of protein stability of FAM49B in LANCL1-KD by shRNA #1 and LANCL1-rescue PLC/PRF/5 cells upon cycloheximide treatment (CHX, 10 μg/ml). Fitting curves show FAM49B protein half-life (left lower) calculated based on the quantification of the FAM49B protein levels relative to β-actin. Ubiquitination of FAM49B protein was examined in the indicated PLC/PRF/5 cells (right). B. The KD efficiency for PSME3 and TRIM21 in PLC/PRF/5 as determined with qPCR (upper). Sphere formation was measured (lower). C. ROS for spheroid cells of the above stable clones. D. Co-immunoprecipitation and immunoblotting of endogenous proteins verified LANCL1, FAM49B, and TRIM21 protein interaction in PLC/PRF/5 cells. E. Protein stability (left) and ubiquitination (right) of LANCL1 and FAM49B in TRIM21-KD PLC/PRF/5 cells. F. FAM49B and TRIM21 proteins were immunoprecipitated in LANCL1-KD or rescue PLC/PRF/5 cells with MG132 treatment to examine the effects of LANCL1 on the binding between FAM49B and TRIM21. *$p<0.05$; **$p<0.01$; ns: not significant.

Figure 6

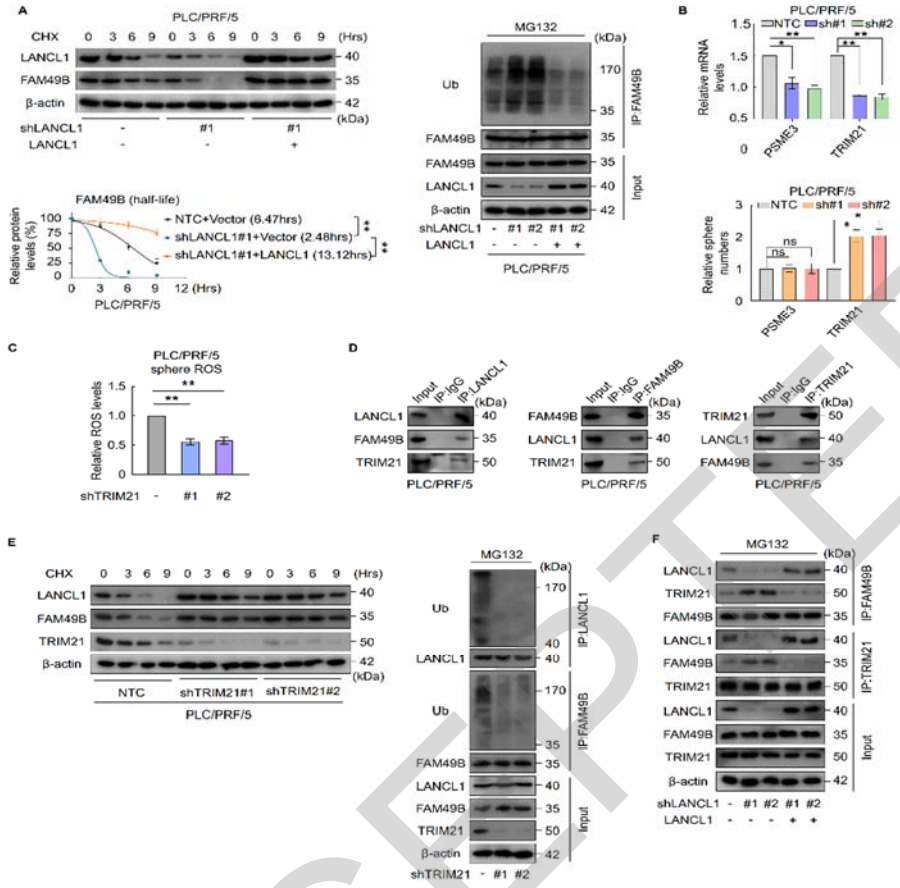

Figure 7. Intracellular C-terminal region of LANCL1 is required for reducing TRIM21-binding to FAM49B and promoting sphere formation inhibited by TRIM21. A. LANCL1 and FAM49B protein levels in PLC/PRF/5 cells with overexpression of TRIM21 and co-overexpression of LANCL1 and TRIM21. B. Sphere formation assays (left) and ROS levels (right) for the above stable clones. C. Limiting dilution assays for the above cells. D. ROS levels were examined in the indicated tumor cells. E. LANCL1 WT or mutants with C-terminal truncations were overexpressed in LANCL1-KD PLC/PRF/5 cells, with results of sphere formation and ROS levels shown. F. Immunoprecipitation of FAM49B and TRIM21 in the indicated PLC/PRF/5 cells and immunoblotting for the indicated proteins. *p<0.05; **p<0.01 ; ns: not significant. Scale bar=200μm.

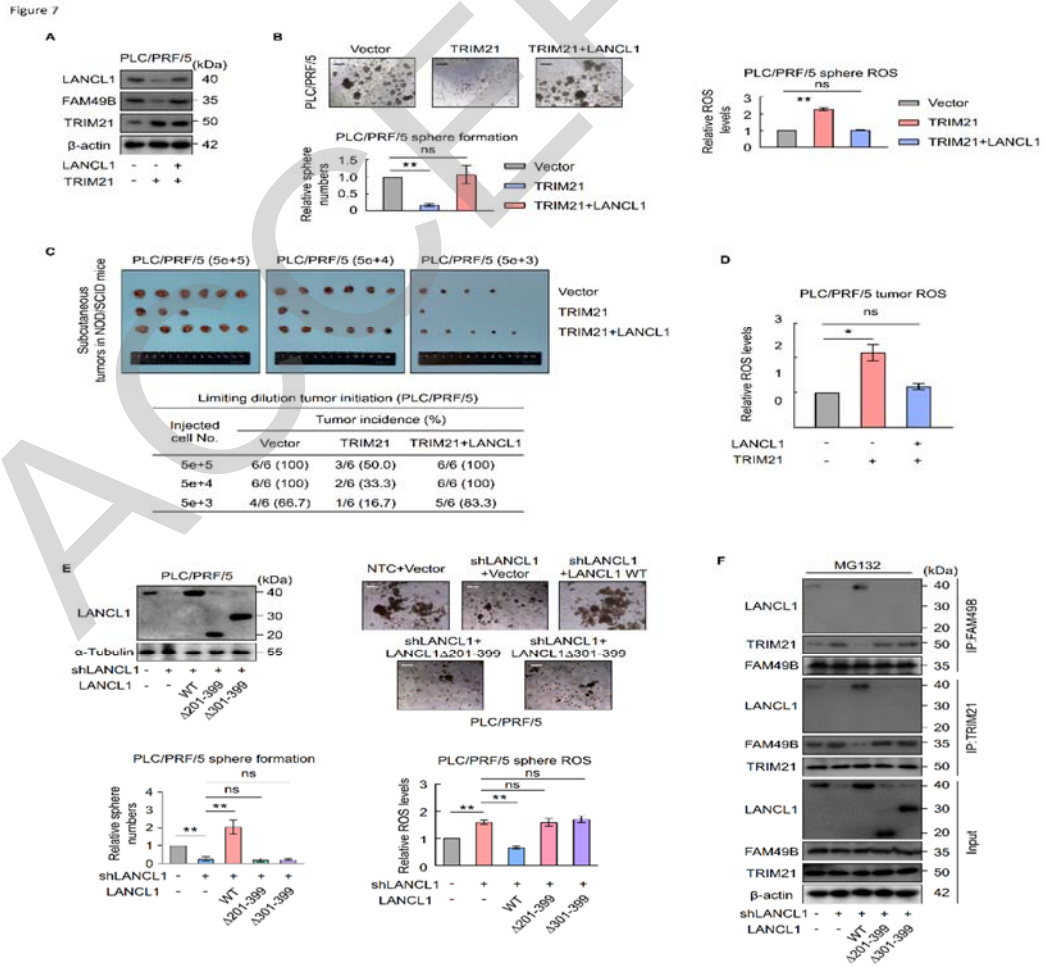

Figure 8. High LANCL1 and FAM49B co-expression is associated with more aggressive tumor behavior and poorer survival.

A. Clinicopathologic correlation analysis by Fisher's exact test for the association between high FAM49B expression (T/NTL >2) and cellular differentiation and tumor stages in HCC subgroups with high and low relative LANCL1 mRNA expression in the paired HCCs and corresponding NTL tissues of the HKU-QMH cohort. B. The overall survival (OS) (left panel) or disease-free survival (DFS) (right panel) based on FAM49B mRNA expression in the HCC subgroup with high relative LANCL1 mRNA expression in the paired HCCs and corresponding NTL tissues of the HKU-QMH cohort. High and low FAM49B expression was defined by T/NTL >2 and T/NTL ≤2, respectively. Remarks: **p < 0.01. C. PLC/PRF/5 cells were treated with LANCL1 antibody (NBP1-81796), targeting 1-47aa epitope, at either 400ng or 800ng, and respective IgG control. Sphere formation was examined. *p<0.05; **p<0.01; Scale bar=200μm. D. LANCL1-FAM49B axis promotes liver tumor initiation by reducing NADPH oxidase (NOX)-mediated oxidative stress. (Upper) In LANCL1-high HCC cells, LANCL1 binding to FAM49B and TRIM21 reduces the interaction between FAM49B and TRIM21 proteins to prevent ubiquitination of FAM49B and enhance FAM49B protein stability, which in turn inhibits activation of Rac1 from GDP to GTP-bound form. With suppressed Rac1 activation, NOX no longer generates ROS. This suppresses oxidative stress and promotes liver tumor initiation. (Lower) However, in LANCL1-low HCC cells or absence of LANCL1 C-terminal region to interact with FAM49B and TRIM21 protein, FAM49B ubiquitination is enhanced for subsequent proteasomal degradation. Rac1

activation is no longer inhibited and hence promotes NOX to generate ROS, resulting in oxidative stress to suppress liver tumor initiation.

Figure 8

A

Correlation analyses between FAM49B mRNA and clinicopathological features in the HCC subgroups with different LANCL1 mRNA levels in the HKU-QMH cohort

Clinical features	Groups	LANCL1 high expression				LANCL1 low expression			
		Total number of cases	FAM49B		P-value	Total number of cases	FAM49B		P-value
			Low	High			Low	High	
Cellular differentiation	I-II	19	14	5	0.035	23	6	17	0.221
	III-IV	25	10	15		23	11	12	
Tumor stage	I-II	14	11	3	0.027	16	5	11	0.752
	III-IV	29	12	17		27	10	17